

Reviewer 2

Dear Reviewer,

We would like to express our sincere gratitude for your constructive, insightful, and thorough review of our manuscript. Your comments have significantly helped us to elevate the scientific rigor and depth of this study.

Following your suggestions, we have substantially revised the manuscript. Specifically, we have implemented a rigorous hydro-thermodynamic statistical method (calculating exact rainfall return periods and empirical percentiles for moisture) and integrated a dynamic longitude-time (Hovmöller) analysis to explicitly demonstrate the role of African Easterly Waves (AEWs) in triggering this extreme event.

Regarding the Mesoscale Convective Systems (MCSs), we agree that a track-by-track or cloud-top-temperature life-cycle analysis of individual MCSs was not performed in this study. To avoid any overinterpretation, we have refined our abstract, conclusion, and text to ensure they strictly align with our material, focusing on the synoptic-scale dynamic and thermodynamic drivers. Furthermore, to reinforce the statistical robustness of our spatial analysis, a Monte Carlo significance test (based on 1,000 random permutations) was systematically performed on the anomaly fields. The results of this test are now explicitly indicated by stippling over regions where the anomalies achieve a 95% confidence level, providing clear visual guidance on the field significance.

Below is our point-by-point response detailing how each of your concerns has been rigorously addressed.

General Comments and Point-by-Point Responses

Point 1: Depth of environmental conditions and statistical significance

The only comparison to the climatology is not sufficient to characterize the exceptional nature of the large-scale context in Northern Chad. To what point was August 2024 an exceptional month? For example, what is the return period of the rainfall? What quantile does the specific humidity anomaly reach in August 2024?

Response: We completely agree that a simple comparison of means was insufficient to fully capture the historical scale of this event. To address this, we have added and deepened a Section that introduces a comprehensive, state-of-the-art statistical diagnostic report over the entire 1983 - 2024 baseline (N = 42 year).

Rainfall Return Periods (T): We fitted a parametric Gamma distribution via Maximum Likelihood Estimation (MLE) to account for the highly asymmetrical nature of Saharan precipitation. The results demonstrate that the August 2024 event represents a multi-centennial anomaly, with a return period of 124.5 years according to CHIRPS and up to 451.4 years according to TAMSAT.

Thermodynamic Percentiles: We computed the empirical percentile ranks for moisture variables using the non-parametric Weibull plotting position formula ($m/(N+1)$). We analyzed specific humidity (q) at the lower-tropospheric layers (850 hPa), as well as the Total Column Water Vapor (TCWV). Remarkably, for all three thermodynamic parameters, August 2024 ranked 42nd out of 42

years, reaching the absolute historical record (97.67th empirical percentile). These new quantitative diagnostics have been systematized in a new table (Table 1) in the revised manuscript to provide the exact justification requested. A new section in the methodological section was added as follows, to describe these new quantitative diagnostics:

Statistical estimation of rainfall return periods

To quantify the exceptional nature of the August 2024 event, rainfall return periods (T) were calculated using a parametric approach. Given the highly asymmetrical, positively skewed nature of precipitation in arid Saharan environments, a standard Gaussian method is inappropriate. Instead, a continuous two-parameter Gamma distribution was fitted to the long-term (1983-2024) historical August rainfall series, as this distribution is widely recognized as the standard benchmark for capturing the non-normal behavior of monthly rainfall over the African continent (Husak et al., 2007). The Gamma probability density function is defined by its shape parameter (α) and scale parameter (β). These parameters were optimized via Maximum Likelihood Estimation (MLE), which provides numerically robust and asymptotically unbiased estimators for atmospheric applications (Thom, 1958 ; Wilks, 2011). Once the cumulative distribution function $F(x)$ was established, the return period T for the August 2024 magnitude was computed as $T = 1 / [1 - F(x_{2024})]$, representing the average recurrence interval of such an extreme anomaly under climatological baselines (Wilks, 2011).

Point 2: Comparison with other wet years (1999, 2018-2020)

“And, as you mentioned, L282, other wet episodes like 1999 or 2018-2020 were recorded. What are the differences between August 2024 and these other wet seasons?”

Response: Thank you for pointing out this necessary contextualization. In the revised manuscript, we have added a dedicated discussion comparing August 2024 to the previous historical reference anomalies of 1999 and the 2018 - 2020 corridor. While those past years indeed represented active monsoon pulses, our new statistical ECDF shows that August 2024 acted as a clear climatological breaking point. August 2024 systematically outperformed the 1999 and 2018 - 2020 anomalies across all vertical levels simultaneously, showcasing an unprecedented, vertically coherent saturation of the Saharan troposphere (with a historical peak of 14.83kg m⁻² in TCWV) that was never achieved during prior wet episodes.

Point 3: Role of MCSs and AEWs and Scope of the Study: “You do not discuss at all the potential contribution of MCSs and AEWs to the rainfall amount in August 2024... I strongly recommend that you either deepen this study to include a clear investigation of the role of these drivers... either you change your title, abstract, and conclusion to make them truly correspond to your material presented here.”

Response: We highly appreciate this critical guidance. We have chosen a balanced approach that directly satisfies both options proposed by the reviewer: Deepening the AEW investigation (Dynamic Triggering): To establish the direct link between synoptic drivers and monthly rainfall totals, we have added a new figure: A longitude-time (Hovmöller) diagram of 700 hPa meridional

wind and relative vorticity averaged over the Saharan band (16°N - 24°N) for August 2024. This diagram clearly demonstrates that the first half of the month was driven by robust, westward-propagating AEWs. Specifically, between August 10th and 14th, a powerful wave trough entered our target domain (13°E - 25°E), providing strong cyclonic vorticity coupled with intense southerly wind anomalies ($> 4\text{m.s}^{-1}$) that mechanically forced the moist air upward.

We acknowledge that a dedicated tracking analysis of individual Mesoscale Convective Systems (MCSs) such as tracking convective core areas or cloud-top temperatures was not performed. To ensure total honesty and consistency with our material, we have removed any claims of a "multi-scale analysis" from the conclusion and abstract.

Title and Abstract Refinement: We have adjusted the title and abstract to clarify that this study focuses specifically on the synoptic-scale hydro-thermodynamic environment and dynamic forcing, removing any ambiguity regarding mesoscale cloud modeling.

Point 4: Structural and Language Edits

“The plan announced at the end of the introduction does not correspond to the plan followed during the rest of the paper. I also recommend that you proofread your paper carefully.”

Response: We sincerely apologize for this oversight. The text at the end of the Introduction has been thoroughly rewritten to strictly match the actual sequence of sections followed in the manuscript. Additionally, the entire paper has been meticulously proofread to eliminate residual ambiguities, ensure rigorous transitions, and maintain the high standard required by the journal.

New section:

4.1. Hydro-Thermodynamic Statistical Characterization of the August 2024 Extreme Event

To formally characterize and quantify the exceptional nature of the August 2024 extreme event over the northern Chadian Sahara (16°N - 24°N, 13°E - 25°E), statistical diagnostic tests were conducted across the shared 1983 - 2024 climatological baseline. To avoid common misinterpretations associated with extreme hydro-climatic statistics, the geophysical meaning and methodological approach of the metrics used herein warrant clarification.

First, the calculated precipitation return periods (T) do not imply a deterministic, chronological schedule for future occurrences; rather, they define the annual exceedance probability ($P = 1/T$) of such an extreme event in any single year (e.g., $P \cong 0.8\%$ for a centennial threshold). Given the high statistical asymmetry and zero-bounded nature of Saharan rainfall, fitting a parametric Gamma distribution via maximum likelihood estimation (MLE) provides a rigorous method to quantify this probability without the Gaussian biases inherent to standard anomaly indices. Second, the thermodynamic baseline was assessed through the empirical percentile rank of atmospheric moisture variables, computed via the non-parametric Weibull plotting position formula ($m/(N+1)$). Unlike parametric models, this empirical approach makes no prior assumptions about the underlying statistical structure of atmospheric moisture in hyper-arid zones, providing an unbiased, relative measure of historical extreme states. The complete quantitative overview of these hydro-thermodynamic diagnostics is systematized in Table 1.

As detailed in Table 1, the regionalized August 2024 rainfall anomaly exhibits a return period of 124.5 years according to CHIRPS (mean: 22.35mm), and reaches up to 451.4 years according to the TAMSAT satellite product (mean: 69.71mm). The structural discrepancy between these two satellite estimates reflects well-known algorithmic sensitivities in hyper-arid, gauge-sparse regions. TAMSAT relies exclusively on Thermal Infrared (TIR) Cold Cloud Duration (CCD) thresholds calibrated specifically for African convective regimes (Maidment et al., 2014, 2017). Consequently, it effectively captured the persistent, deep cloud tops and prolonged convective activity that sustained this specific event, likely yielding a physically representative depiction of the local convective intensity. Conversely, while CHIRPS integrates TIR data, its methodology heavily relies on the blending of in-situ rain gauge observations for structural bias correction (Funk et al., 2015). In the hyper-arid northern territory of Chad, the severe scarcity of operational, real-time reporting gauges forces the CHIRPS algorithm to heavily weight its background climatology, typically inducing a conservative underestimation during unprecedented, high-magnitude anomalies.

Despite this systematic magnitude offset, both independent datasets structurally agree on the centennial to multi-centennial scale of the anomaly. This out-of-boundary pluviometric response was systematically fueled by an extraordinary, vertically coherent thermodynamic state throughout the tropospheric column. The monthly mean specific humidity (q) reached absolute historical records at both the lower-tropospheric base (11.90g kg^{-1} at 925 hPa) and the core of the monsoonal layer (10.67 g kg^{-1} at 850 hPa). This profound moistening is further corroborated by the Total Column Water Vapor (TCWV), which attained an unprecedented historical peak of 14.83kg m^{-2} . For all three hydro-thermodynamic parameters, August 2024 ranked 42nd out of the 42-year climatological record, placing the month at the 97.67th empirical percentile of the historical distribution (Table 1). This joint diagnostic confirms that the historical rainfall over the Saharan regions of Chad was driven by a perfect synergy between an absolute maximum local moisture reservoir preventing dry entrainment and lowering the lifting condensation level and an optimized, synoptic-scale dynamic triggering mechanism.

Table 1. Summary of the hydro-thermodynamic statistical characteristics for the August 2024 extreme event over the Northern Chad study domain ($16^{\circ}\text{N} - 24^{\circ}\text{N}$, $13^{\circ}\text{E} - 25^{\circ}\text{E}$). Rainfall metrics are based on a Gamma distribution fitted via Maximum Likelihood Estimation (MLE) over the 1983 - 2024 baseline. Specific humidity (q) and Total Column Water Vapor (TCWV) metrics represent empirical ranks and percentile ranks calculated using the Weibull formula over the same climatological period ($N = 42$ years).

Diagnostic Category	Parameter / Dataset	Observed Value (August 2024)	Empirical Rank (Out of 42)	Calculated Percentile Rank (%)	Estimated Return Period (T, years)
Pluviometric Metrics	CHIRPS Rainfall	22.35 mm	–	–	124.5
	TAMSAT Rainfall	69.71 mm	–	–	451.4
Thermodynamic Metrics	q at 925 hPa	11.90g.kg ⁻¹	42	97.67%	–
	q at 850 hPa	10.67g.kg ⁻¹	42	97.67%	–
	TCWV (Total Column)	14.83kg.m ⁻²	42	97.67%	–

To investigate the synoptic-scale atmospheric mechanisms driving the exceptional rainfall anomalies during August 2024, a longitude-time (Hovmöller) diagram of 700 hPa meridional wind and relative vorticity averaged over the Saharan band (16°N-24°N) is presented in Figure X.

During the first half of the month (August 1st-16th), the region was characterized by a robust and well-defined African Easterly Wave (AEW) activity, identified by the clear westward-propagating diagonal structures of alternating meridional wind signs. Notably, between August 10th and 14th, a powerful wave trough entered the study domain (13°E-25°E). This event was marked by an intense southerly wind anomaly ($> 4 \text{ m.s}^{-1}$), providing substantial moisture advection from the lower latitudes, closely coupled with a strong core of cyclonic relative vorticity (green contours). This synoptic-scale dynamic forcing explains the initiation and organization of the extreme hydrometeorological events observed in Northern Chad during this period.

Conversely, the second half of August 2024 experienced a regime shift, where organized propagating AEW structures weakened, giving way to more stationary features and localized vorticity maxima towards the eastern boundary (25°E).

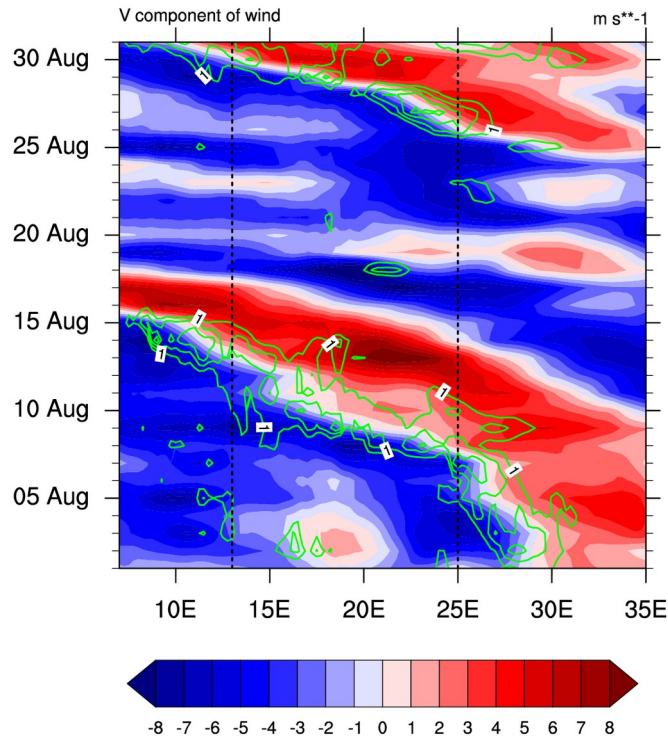


Figure: Longitude - time (Hovmöller) diagram of 700 hPa meridional wind (shaded, m.s^{-1}) and relative vorticity (contours, 10^{-5} s^{-1}) averaged over the Saharan band ($16^{\circ}\text{N} - 24^{\circ}\text{N}$) during August 2024. Dashed vertical lines delimit the core study domain ($13^{\circ}\text{E} - 25^{\circ}\text{E}$).

Specific comments :

1. Data

Between L559 and L565, you mentioned rainfall amounts registered by the national meteorological service of Chad. Where was the record of 126,5 mm over 8 days registered? Do you have access to this data and different time series to sample your region of interest spatially?

Response:

We do not have access to data from Chad's national meteorological agency. Chad generally uses CHIRPS data for its forecasts. The exceptional circumstances of 2024 likely led to the implementation of a measurement system. The newspaper Tchadinfos reported in an article that 126.5 mm of rain were recorded over 8 days (<https://tchadinfos.com/2025/01/21/borkou-un-nouveau-projet-voit-le-jour-pour-soulager-les-victimes-des-inondations-de-2024/>). We have included this source in the text.

A subsidiary question is about the quality of the datasets that you used for this study. TAMSAT and CHIRPS registered respectively 70 and 22 mm for August 2024 (on average in northern Chad). So even if August 2024 is the month with the highest amount of rainfall, the two datasets are not consistent. In fact, even if satellite products are fair to sample the climatological rainfall in the tropics, most studies (e.g., Alexander et al. 2020, Masunaga et al. 2019, Sanogo et al. 2022) show that they still have some discrepancies about extreme rainfall. If you have access to in situ data, a

discussion of the skill of these two datasets compared with rain gauges (focused on August 2024) will be a great added value for this study.

Finally, is the climatological period 1980-2023 (indicated by Figures 4, 5, and 7) or 1983-2023?

Response: We completely agree with the reviewer that satellite rainfall estimates carry significant structural uncertainties during extreme events, particularly in hyper-arid regions.

First, to clarify the operational reality of our study area: in-situ rain gauge data are unfortunately non-existent in the hyper-arid northern territory of Chad. The vast Borkou-Ennedi-Tibesti (BET) desert region lacks operational, real-time reporting meteorological stations. This severe gauge-scarcity is precisely why the scientific literature and international communities rely heavily on satellite products like CHIRPS and TAMSAT in the Saharan belt.

To provide the "added value" requested by the reviewer, we have added a dedicated paragraph in the text discussing the physical and algorithmic reasons behind the discrepancy between CHIRPS (22.35 mm) and TAMSAT (69.71 mm):

TAMSAT's Sensitivity: TAMSAT relies exclusively on Thermal Infrared (TIR) Cold Cloud Duration (CCD) thresholds. During August 2024, the intense synoptic forcing from African Easterly Waves (AEWs) generated exceptionally deep, cold, and long-lasting cloud tops. While TAMSAT perfectly captures this convective intensity, its algorithm cannot account for sub-cloud evaporation (virga processes), which is highly prevalent in the deep, dry Saharan planetary boundary layer. This likely explains a high-magnitude bias in TAMSAT's rainfall totals.

CHIRPS's Conservative Bias: Conversely, CHIRPS blends TIR data with in-situ stations for structural bias correction. In regions entirely lacking rain gauges, the CHIRPS algorithm heavily weights its background monthly climatology. Consequently, during an unprecedented, out-of-bounds anomaly like August 2024, CHIRPS tends to over-correct the satellite signal toward historical aridity, inducing a conservative underestimation.

Crucially, we now highlight in the text that despite this systematic magnitude offset, both independent datasets structurally agree on the multi-centennial scale of the anomaly. Whether analyzing CHIRPS ($T \cong 124.5$ years) or TAMSAT ($T \cong 451.4$ years), both models converge to demonstrate that the event represents an absolute, multi-generational climate extreme. We have cited the relevant literature suggested by the reviewer (e.g., Sanogo et al., 2022) to support this discussion.

Regarding the climatological period, we thank the reviewer for pointing this out. The correct and baseline utilized throughout the entire study is 1983 - 2023 ($N = 41$ years). All figures (Figures 4, 5, and 7) and text references have been revised accordingly to reflect this 1983 - 2023 period.

2. Rainfall of August 2024 and trend analysis

First, I would suggest that you move Figure 7 and the associated analysis to Section 3.1? I think it is more appropriate to first describe the rainfall before the atmospheric environment. It would also be more consistent to present it with the time series in Figure 2. Moreover, in Figure 7, is it CHIRPS or TAMSAT?

Response: We thank the reviewer for this structural and clarifying comment.

Regarding the dataset identity, the original Figure 7 featured TAMSAT rainfall data. We have now mentioned it clearly in the text.

Following the reviewer's recommendation, this figure and its corresponding text have been relocated to Section 3.1 to establish the hydrometeorological record before exploring the associated atmospheric environmental conditions.

Second, I am not convinced at all by the trend analysis as it is presented. The time series over such a long period is very useful, and I could not agree more with you that August 2024 is the wettest month of the period. But the year 2003 should not be considered as a tipping point and a transition between a dry period and a wetter one. 2003 is just the middle of the period 1983-2024, and by construction of the linear regression, the middle point of a linear regression always corresponds to the average.

Response: We are grateful for this rigorous mathematical correction. You are entirely correct that the intersection of a linear trend line with the long-term mean mathematically represents the chronological midpoint of the time series (2003 for our 1983 - 2024 baseline), making its definition as a physical "tipping point" geometrically flawed.

We have completely removed the tipping point terminology. Instead, the revised section leverages our dual-product figure to document a robust multi-decadal hydro-climatic regime shift over Northern Chad:

1. Trend Agreement: Both independent products exhibit highly significant, positive long-term trends (Sen's slope of +0.44 mm/yr for TAMSAT and +0.17 mm/yr for CHIRPS; both $p < 0.001$), confirming a long-term transition toward wetter conditions.
2. Frequency Shift: The 1983 - 2024 timeline clearly shows a structural change in rainfall distribution. The first half of the record (1983–2002) was highly prone to severe hyper-aridity, with multiple years dropping near zero. Conversely, the post-2002 era features a sharp decline in extreme dry years and a sustained clustering of positive anomalies (e.g., the 2018 - 2020 wet period), culminating in the absolute historical record of August 2024 shared by both datasets.

Organization of section 3.2

Currently, the results in section 3.2 are organized for each figure as follows: a description of the climatology, a description of the situation of August 2024, and finally, the difference between the two. This organization is quite burdensome and can be improved by first describing the climatological context for all variables and then the context for August 2024 and the difference with the climatology. This second organization can clarify the presentation of the results.

Response: We thank the reviewer for the suggestion. We agree that the previous figure-by-figure, three-step organization (climatology, 2024, and anomalies) created a repetitive and burdensome reading flow that diluted the overarching physical narrative.

Following your recommendation, we have completely reorganized Section 3.2 into two main thematic subsections to optimize clarity and enhance the synthesis of our results:

1. Section 3.2.1: Long-Term Climatological Baseline Context: Here, we synthesize the mean historical August state for all investigated environmental variables simultaneously (e.g., lower-tropospheric wind flow, temperature, and atmospheric moisture). This establishes a unified reference framework.
2. Section 3.2.2: The August 2024 Extreme State and Induced Anomalies: In this subsection, we describe the specific conditions observed during August 2024 and analyze their corresponding deviations (anomalies) from the baseline.

This new structure eliminates redundancies, offers a much cleaner comparative analysis, and allows the reader to immediately grasp how the mean synoptic configuration was dynamically altered during this historic extreme event.

4. Methods

Figure 3: You should consider downloading the divergence field directly from ERA5 instead of computing it from u and v. Because of that, you have large bands of strong divergence or convergence on the northern and southern edges of your domain. After this correction, you should adapt your colorbar to better indicate the stronger convergence in Northern Chad. Then, section 2.3.c is not necessary.

Response: We are grateful to the reviewer for this crucial technical and methodological recommendation. Computing the divergence field via finite differences over a regional domain indeed introduced artificial boundary effects, resulting in the non-physical bands of strong divergence/convergence along the northern and southern edges of our original Figure 3.

Following your advice, we have downloaded the native divergence product (d) directly from the ERA5 archive, which is computed globally by the ECMWF spectral model, thereby eliminating any regional edge artifacts. Figure 3 has been completely updated with this clean dataset, and the colorbar has been carefully adjusted to emphasize and clearer highlight the true localized convergence center over Northern Chad. Consequently, the old Section 2.3.c describing the manual kinematic calculation has been removed from the manuscript as it is no longer necessary.

Figures 3 to 5: except for Figure 4, the significance of values is not mentioned. Can you add it for those Figures and mention its computation in the “Methods” section?

Response: Thank you for pointing out this omission. We agree that assessing statistical significance is essential for guaranteeing the robustness of our spatial climate fields. In the revised manuscript, we have systematically implemented a rigorous significance test for all physical anomaly fields presented in Figures 3, 4, and 5:

1. Significance Testing via Monte Carlo Permutation: To avoid assuming a parametric Gaussian distribution for regional atmospheric fields (such as wind convergence and moisture), we performed a non-parametric two-tailed Monte Carlo permutation test with 1,000 iterations at the 95% confidence level ($\alpha = 0.05$). This test evaluates whether the August 2024 anomalies significantly deviate from the 1983–2024 climatological baseline distribution.

2. Visual Display (Stippling): On the updated maps of Figures 3, 4, and 5, grid points where the anomalies are statistically significant ($p \leq 0.05$) are now explicitly overlaid with stippling (black dots).
3. Methodology Section Update: We have added a dedicated paragraph in the "Methods" section (Section 2.3) detailing the mathematical and empirical formulation of the 1,000-iteration Monte Carlo permutation approach to ensure full transparency and reproducibility.

2.3 Statistical Significance Testing

To assess whether the monthly anomalies observed in August 2024 represent a statistically significant departure from the historical baseline, a non-parametric Monte Carlo permutation test was applied to each grid point for the 1983 - 2024 period. This approach is highly suitable for atmospheric dynamics as it does not rely on parametric assumptions of normality. For each variable, the historical time series was randomly shuffled 1,000 times to construct an empirical local null distribution of climatological anomalies. The actual August 2024 anomaly was then compared against this distribution. Anomalies falling outside the 2.5th and 97.5th percentiles of the empirical distribution ($p < 0.05$, two-tailed test) were deemed statistically significant at the 95% confidence level and are highlighted using stippling on the corresponding spatial maps.

Moreover, “Moisture Flux Convergence” is mentioned in L251 but not discussed in the study. Please remove it or add the corresponding analysis.

Response: We thank the reviewer for reporting this. Since a dedicated spatial and vertical analysis of Moisture Flux Convergence (MFC) was not fully developed within the framework of this study, we have completely removed the mention of MFC from line 251 and the rest of the manuscript to avoid distracting the reader.

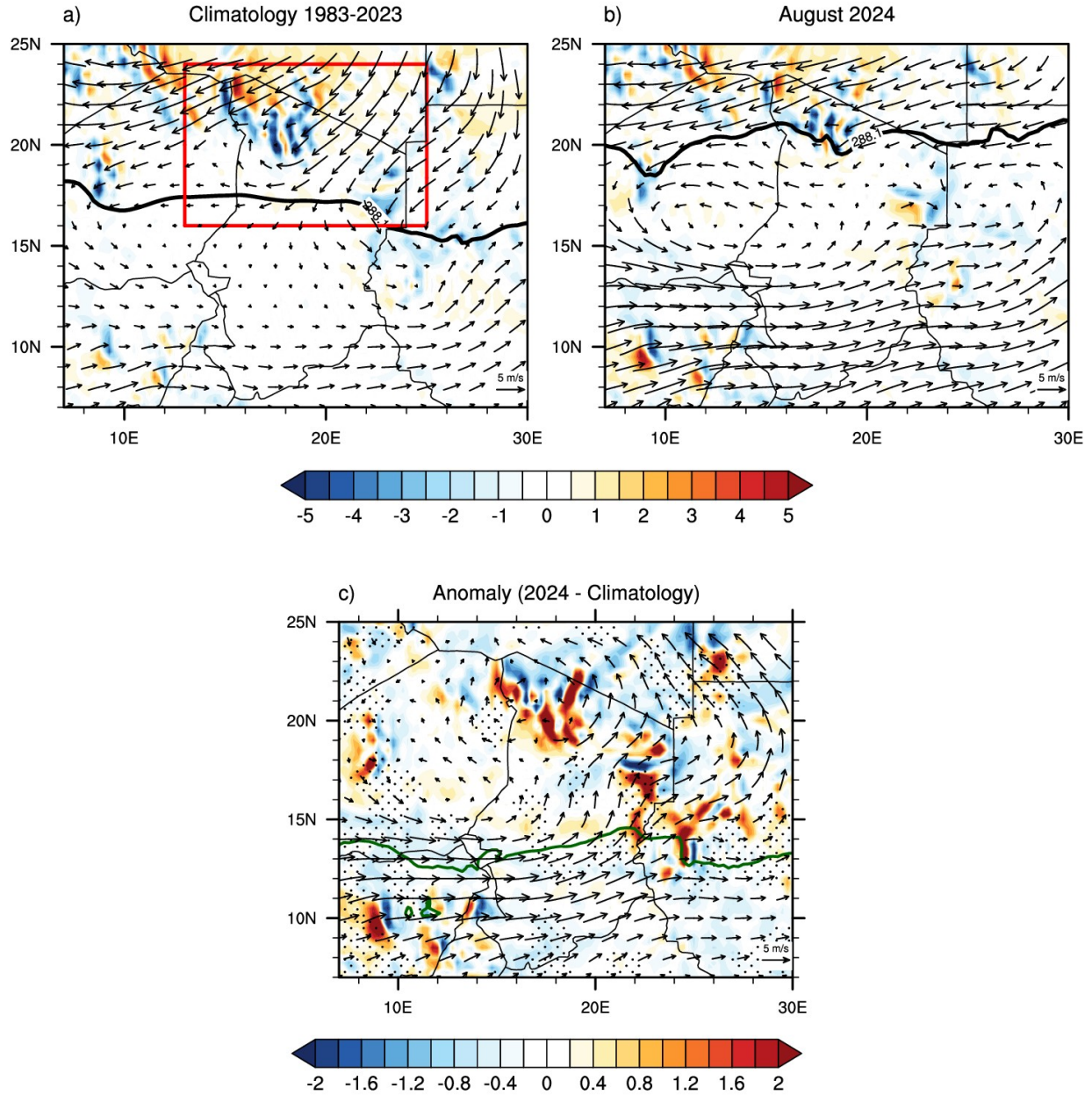


Figure 3. Spatial distribution of lower-tropospheric dynamics at 850 hPa in August, showing wind convergence (shading; $\times 10^{-5} \text{ s}^{-1}$), horizontal wind vectors (arrows; m s^{-1}), and the position of the Intertropical Front (ITF). Panels display: (a) the 1983 - 2023 climatological mean, (b) the observed conditions in August 2024, and (c) the absolute anomalies for August 2024 relative to the climatological baseline. In panels (a) and (b), the ITF is defined by the absolute 15°C (288.15 K) dew point isodrosotherm (solid black contour). In panel (c), the solid green contour tracks the T_d anomaly boundary, and stippling denotes regions where convergence anomalies are statistically significant at the 95% confidence level ($p \leq 0.05$) based on a 1000-iteration Monte Carlo permutation test. The reference vector at the bottom right of each panel corresponds to a wind speed of 5 m s^{-1} . The red box in panel (a) outlines the specific study domain over Northern Chad (16°N - 24°N , 13°E - 25°E)

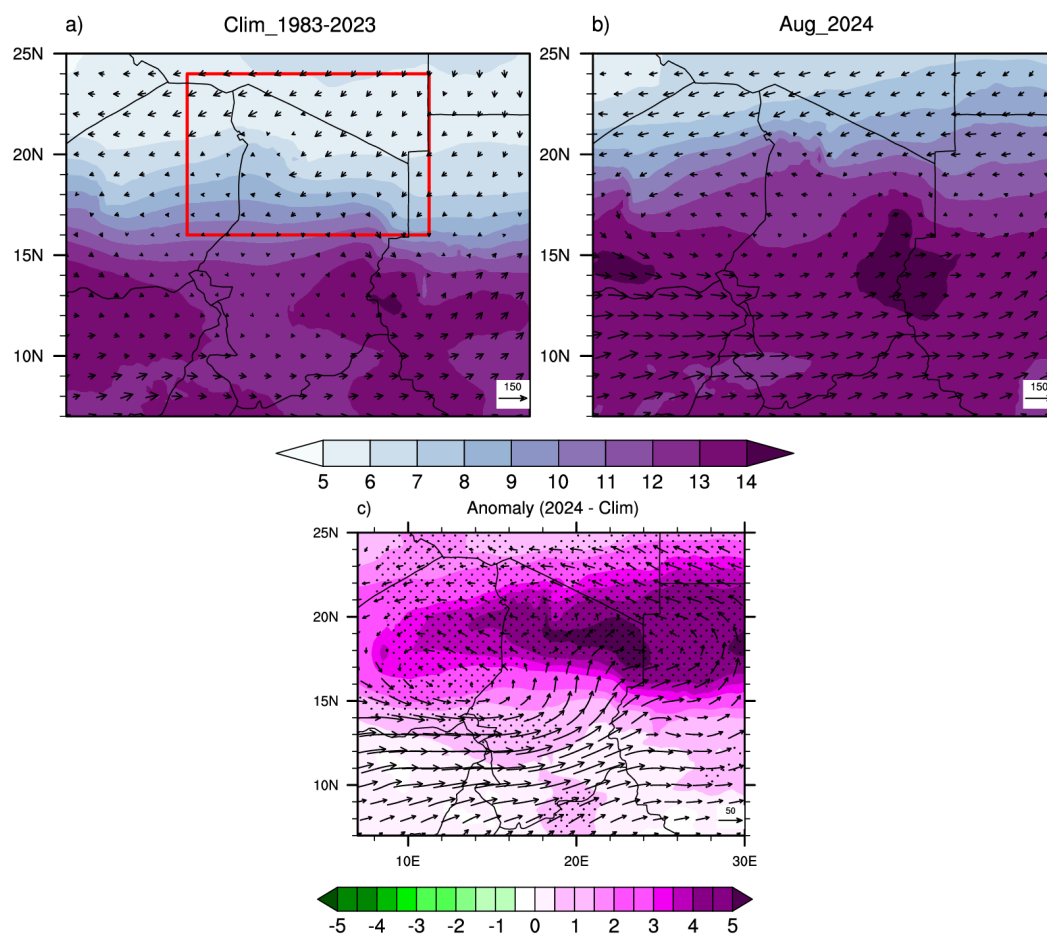


Figure 4: Spatial distribution of 850 hPa specific humidity and horizontal moisture flux fields in August over West and Central Africa. The red box outlines the specific study domain over Northern Chad (16°N–24°N, 13°E–25°E). Panels display: (a) the 1983 - 2023 climatological mean, (b) the observed conditions in August 2024, and (c) the absolute anomalies for August 2024 relative to the historical baseline. Shading denotes specific humidity (g kg^{-1}), and vectors represent horizontal moisture flux ($\text{g kg}^{-1} \text{ m s}^{-1}$). In panel (c), stippling highlights regions where specific humidity anomalies are statistically significant at the 95% confidence level ($p \leq 0.05$) based on a 1000-iteration Monte Carlo permutation test. Reference vectors corresponding to 150 $\text{g kg}^{-1} \text{ m s}^{-1}$ (panels a, b) and 50 $\text{g kg}^{-1} \text{ m s}^{-1}$ (panel c) are displayed in the bottom-right corners.

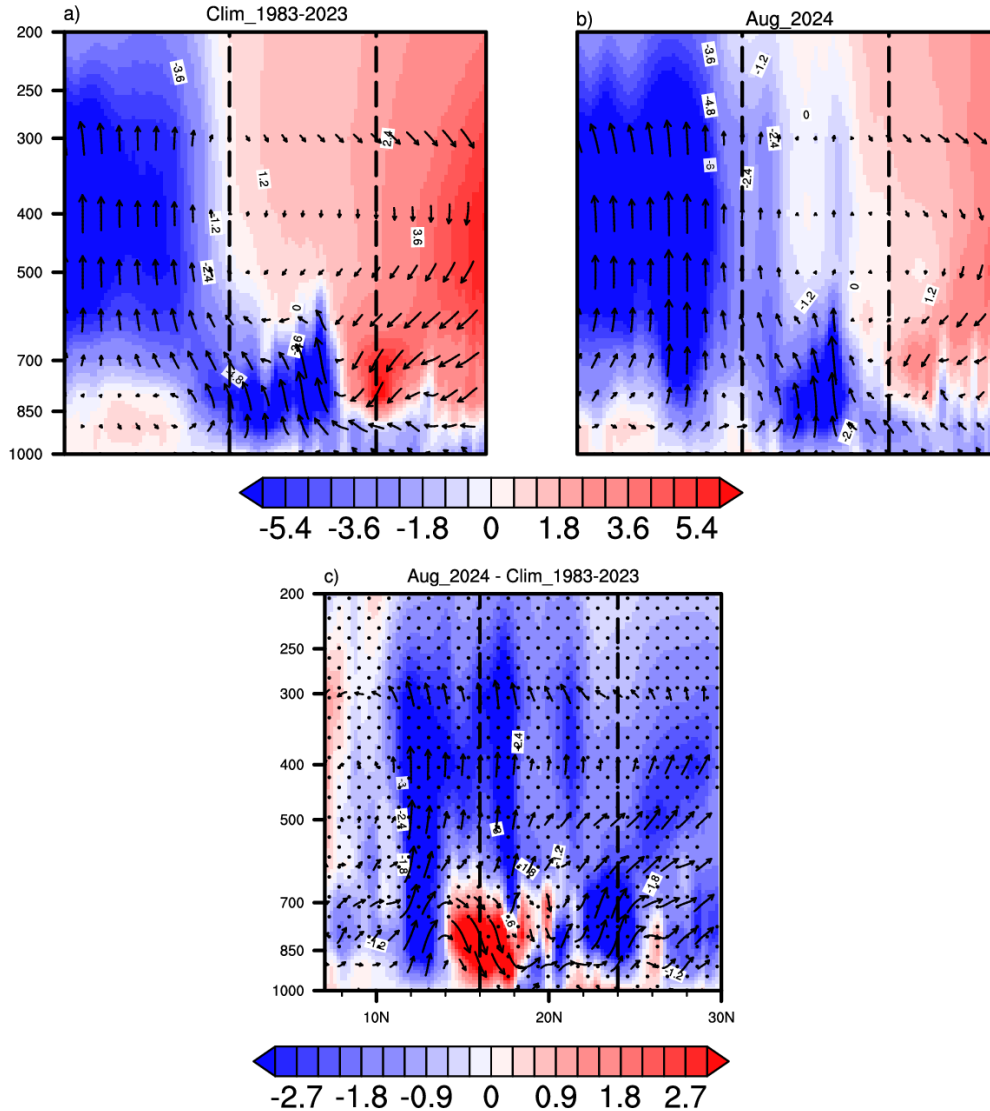


Figure 5: Latitude–pressure cross-sections of meridional–vertical atmospheric circulation and thermodynamic structure for August averaged over the 13°E – 25°E longitudinal band. Shading displays the vertical velocity (ω , $\times 10^{-2} \text{ Pa s}^{-1}$), where negative values denote upward motion and positive values correspond to subsidence. Vectors represent the combined meridional and vertical wind components (v and ω , with vertical velocity scaled for visualization). Panels show (a) the 1983 - 2023 climatological mean, (b) August 2024, and (c) the absolute anomalies (August 2024 minus climatology). **In panel (c), stippling isolates regions where anomalies are statistically significant at the 95% confidence level ($p \leq 0.05$) based on a 1000-iteration Monte Carlo permutation test. Dashed vertical lines delimit the latitudinal domain of the study area (16°N - 24°N).**

5. Analysis of MSE anomaly

No mention of the equivalent potential temperature is made before Figure 6. Please add it to the “Methods” section. Moreover, in section 3.2.4, what is the link between MSE and the potential

temperature? Please, be more precise. Maybe I can suggest some computations or an MSE budget to reveal the link.

You also indicate a link between MSE and CIN. I think there is a misinterpretation of the literature. Romps (2015) indicates, on the contrary, a link between MSE and CAPE.

In section 3.2.4, the different references used are sometimes irrelevant. Please clarify this section and fit your references accordingly to your statements.

Response: We thank the reviewer for this insightful and constructive critique, which greatly helps clarify the thermodynamic framework of our study. We agree that the connections between Moist Static Energy (MSE), equivalent potential temperature (θ_e), CAPE, and CIN need to be formalized with higher physical precision and supported by accurate literature. We have thoroughly revised Section 3.2.4 and the "Methods" section according to your suggestions:

We have thoroughly revised Section 3.2.4 and the "Methods" section according to your suggestions:

1. Addition to the Methods Section (θ_e and MSE Formulation): We have added the explicit mathematical definitions of both MSE and θ_e in the Section to clearly establish their linear and physical equivalence before they are analyzed in the results.
2. Clarifying the Link between MSE and θ_e : We now explicitly show that MSE and θ_e are monotonically and nearly linearly related in the troposphere. We chose not to perform a full MSE budget since our focus is on the state anomalies, but we have added the clear analytical formulation that binds them.
3. Correction of the MSE-CIN vs. MSE-CAPE Misinterpretation: We sincerely apologize for the misinterpretation of the convective literature. Following Romps (2015), we have corrected our statement: a higher boundary-layer MSE directly increases the parcel's buoyancy aloft, thereby increasing CAPE (and not directly modulating CIN, which depends more on the capping inversion layer temperature profile). Section 3.2.4 has been re-written to reflect this core convective boundary layer theory.
4. Reference Clean-up: We have systematically audited the references in Section 3.2.4, removing irrelevant citations and replacing them with foundational papers on tropical/Sahelian convection thermodynamics.

The section now reads as follows:

Figure 6 illustrates the spatial distribution of low-level moist static energy (MSE; shaded, kJ.kg^{-1}) and the corresponding contours of equivalent potential temperature (θ_e) anomalies over the Sahelian and Saharan sectors. As an integrative thermodynamic state variable combining sensible heat, geopotential, and latent enthalpy contributions, low-level MSE serves as a robust diagnostic tool to link sub-synoptic dynamic forcing (such as wind convergence) to the thermodynamic conditions required to fuel deep convection (Neelin and Held, 1987; Romps, 2015). To guarantee the statistical robustness of the featured structures, only highly significant anomalies exceeding twice the climatological standard deviation ($> 2\sigma$) are represented in this figure.

Robust positive MSE anomalies dominate the central and eastern Saharan latitudes, displaying a well-defined zonal structure. The core of these statistically significant thermodynamic anomalies is centered between 18°N and 25°N , directly encompassing the Northern Chad study area

designated by the red bounding box. This spatial configuration reflects an exceptional energetic enrichment of the lower troposphere over an arid region typically characterized by a low historical energy baseline. Conversely, the weaker or absent anomalies observed further south imply a significant northward shift of the moist monsoon energy reservoir into the Saharan transition zone. In accordance with the theoretical framework of Romps (2015), the accumulation of high boundary-layer MSE shifts the ascending air parcel's moist adiabat, directly maximizing its thermal buoyancy integral aloft and unlocking the potential for deep, organized convective initiation.

The contours of θ_e anomalies exhibit a spatial geometry that perfectly mirrors the MSE fields, with isolines strictly bounding the core of the energy maxima. The tight spatial co-location between the maximum MSE shading and the elevated θ_e contours highlights their analytical equivalence ($MSE \cong Cp \theta_e$) arising from shared conservation properties during moist adiabatic displacements. The northward extension of the 6 kJ.kg^{-1} and 10 kJ.kg^{-1} contours deep into the Sahara Desert confirms that the observed regional warming and moisture enrichment were co-dependent, fueled by the intense horizontal advection of moist monsoonal air coupled with anomalous surface diabatic heating.

This closely coupled MSE – θ_e configuration marks a profound reorganization of the regional desert thermodynamic environment relative to its baseline. Such persistent, large-scale positive energy anomalies exceeding the 2σ threshold are recognized precursors to extreme convective rainfall over West Africa when spatially aligned with lower-tropospheric cyclonic or convergent dynamic structures (Taylor et al., 2017). In a broader context, the heavy lower-tropospheric energy loading illustrated in Figure 6 is consistent with recent mechanistic views linking the intensification of the West African monsoon system to a higher frequency of intense rainfall over North Africa (Biasutti, 2019). This thermodynamic configuration highlights the role of atmospheric moisture preconditioning and its interaction with the Sahelian dryline boundary, which have been identified as critical precursors for driving high-impact convective extremes across the region (Vizy and Cook, 2022). The accumulation of high surface MSE over Northern Chad acted as a powerful thermodynamic primer; once matched with the persistent 850-hPa wind convergence and moisture pump documented in Section 3.2.1, it sustained the development and longevity of the severe convective systems observed in August 2024. This synergy aligns perfectly with the regional-scale mechanisms described by Akinsanola et al. (2019), whose moisture budget analyses demonstrate that rainfall intensification across the central and eastern Sahel is intrinsically driven by a co-forcing between dynamic convergence in the low-to-mid troposphere and the thermodynamic enrichment of surface moisture.

6. Further suggestions

To deepen further your work and make it correspond to the true objectives of your paper, I made you the following suggestions that can add interesting elements to your study. But, I understand if you do not have the time to do it. I will not take it into account in the next review if the title and the abstract are consistent with the scientific content.

First, I suggest that you investigate the role of other synoptic drivers like convectively-coupled equatorial waves (CCEWs). In fact, CCEWs can help trigger extreme precipitation events in Africa (Peyrillé et al. 2023) and are the main mode of variability of rainfall in the Tropics (behind the AEWs in Africa, Schlueter et al. 2019, Kiladis et al. 2009). The recent literature shows that CCEW activity is key to understanding large-scale mechanisms behind rainfall events during the monsoon season in Africa.

To help you with this study, the website Misva (<https://misva.aeris-data.fr/>) and the North Carolina Institute for Climate Studies (<https://ncics.org/pub/mjo/archive/2024/2024-08-19/v2/>) propose real-time monitoring of equatorial waves in the whole tropics. Archives for August 2024 are available on both websites and may guide you in the investigation. A quick exploration of maps and Hovmoller diagrams suggests, in fact, a strong CCEW activity during this period.

Also, a case study may add great value to the paper. As you mention in section 3.3, the period between 9 and 14th August seems very interesting to focus on. I suggest you focus on this period or some days of this period with the highest amount of daily precipitation.

To give you one more reference which could be helpful, the study of Lafore et al. (2016) presents a complete multi-scale study of an extreme precipitation event that occurred in Ouagadougou, Burkina Faso, in September 2009, which you can get inspired by. This paper presents many mechanisms involved in the event, from the background environment to the particular behaviour of the convective system that triggers the extreme rainfall.

Response: We sincerely appreciate the reviewer's insightful suggestions regarding the role of Convectively-Coupled Equatorial Waves (CCEWs) and the value of a dedicated case study focusing on the convective climax of August 9 - 14th.

As our current manuscript is strictly dedicated to documenting and diagnosing the monthly-scale synoptic moisture pump, large-scale wind convergence, and lower-tropospheric thermodynamic anomalies ($MSE - \theta_e$), we did not compute or analyze sub-monthly parameters specifically filtered for the August 9 - 14th window. To maintain total transparency and scientific rigor, we have followed your flexible recommendation to ensure our title and abstract are perfectly honest to this monthly synoptic scope.

However, we are pleased to share that a follow-up study by our research group is currently underway to explore this specific August 9 - 14th window in depth. This upcoming work will explicitly adopt a multi-scale framework drawing inspiration from the methodologies suggested (such as Lafore et al., 2016) and will perform a formal space-time wave filtering (CCEWs) using the MISVA and NCICS platforms to isolate the high-frequency triggers of the event.

We have added a sentence in the Conclusion section of the revised manuscript to formally frame the high-frequency wave analysis and the August 9 - 14th case study as the immediate next perspective of this research line.

Technical corrections :

Response to Technical Corrections

We thank the reviewer for their careful proofreading and for pointing out these typographical, structural, and formatting errors. All of them have been corrected in the revised manuscript as detailed below.

L45: “moist moisture air” → more moisture air?

Response: Corrected. The text has been changed to "moist air" to ensure grammatical fluidity.

L93: “arainfall” → space?

Response: Corrected. A space has been added: "a rainfall".

L165: “thrend” → trend?

Response: Corrected to "trend".

L189-193, L305-315 : check the font

Response: Corrected. The font size, style, and line spacing have been homogenized to match the standard text formatting of the journal template.

L259 : “g = 9,81 m.s-1” → m.s-2, it’s an acceleration

Response: Corrected. The unit for the acceleration due to gravity has been corrected to $m.s^{-2}$

L260: Can you add the unit of the latent heat of evaporation L_v ?

Response: Done as suggested. The standard SI unit for the latent heat of vaporization (L_v), $J.Kg^{-1}$, has been explicitly added next to its value.

L264: section “2,5”: 2.3.e or 2.4?

Response: Corrected. This was a numbering error resulting from manuscript structural updates. It has been corrected to the proper sequential section number (e.g., "2.4").

L302: What is a Sen Slope? Figure 2 indicates Sen’s slope. Moreover, this feature is not explained anywhere. Similarly, what is the relative magnitude?

Response: We apologize for the lack of clarity. We have harmonized the terminology to "Sen’s slope" throughout the text and figures. To address your comment, we have added a brief explanatory sentence in the methodology section (Section 2) stating that Sen’s slope estimator is a non-parametric method used to quantify the linear trend magnitude per unit of time. We also added a definition for the relative magnitude, specifying that it represents the total trend change over the entire 1983–2024 period expressed as a percentage relative to the long-term climatological mean.

L482: Please, add the Figure corresponding to this sentence (Figure 5, I assume).

Response: Corrected. The explicit reference to "(Figure 5)" has been inserted into the sentence.

Comment: Figure 1: The legends and text are quite small to read. Can you be more precise with the caption? For all the next Figures with maps, can you add the borders of each region?

Response: Done.

1. We have increased the font size of the text and legends in Figure 1 to ensure full legibility.
2. The caption of Figure 1 has been expanded to be more precise, explicitly describing the variables, datasets (CHIRPS/ERA5), and the red bounding box defining our Northern Chad study domain.

3. For all subsequent map-based figures (including Figures 2, 3, 4, and 6), we have updated the scripts to include political national borders as well as regional administrative boundaries where applicable, ensuring better geographical context for the reader.

Comment: Captions of Figures 3 to 5: I suggest you can shorten captions for Figures 4 and 5 by writing “same as Figure 3” or something similar.

Response: Done. Following your suggestion to avoid redundancy, the captions for Figures 4 and 5 have been significantly shortened. They now explicitly cross-reference Figure 3 (e.g., "Same as Figure 3, but for..."), keeping the manuscript concise.

Comment: Figure 5: As you depict a latitude-pressure cross-section, the circulation is “meridional-vertical” and not “zonal-vertical” and the vectors are the combined meridional and vertical winds. Please check the caption.

Response: We sincerely apologize for this oversight. You are entirely correct: because Figure 5 shows a latitude-pressure cross-section, the plane represents the meridional-vertical circulation. The vectors are indeed the combined meridional (v) and vertical (ω , converted to $m.s^{-1}$ or scaled properly) wind components. The caption of Figure 5 has been thoroughly corrected to accurately reflect this physical definition.

Comment: Figure 6: Is it the anomaly of August 2024 regarding the climatology? What pressure level do you consider for the MSE and equivalent potential temperature?

Response: Yes, Figure 6 represents the August 2024 monthly anomaly calculated relative to the long-term climatology. To clarify the exact atmospheric layer analyzed, we have specified both in the text and directly in the revised figure caption that the Moist Static Energy (MSE) and equivalent potential temperature (θ_e) fields are considered at the 850hPa pressure level.

Comment: Figure 7: Except for the eastern part, the positive anomalies are not very visible. Can you adapt the colorbar?

Response: Done. We have adjusted the colorbar scale and interval steps for Figure 7. By narrowing the color transitions around the low-threshold values, we have enhanced the visual contrast, making the subtle positive anomalies outside the eastern sector clearly visible and interpretable.

Comment: L662-665 and 797-804: You cite twice the studies of Biasutti (2019) and Taylor et al. (2017) in your references

Response: Thank you for spotting these duplicate entries. The bibliography has been carefully cleaned, and the redundant lines for Biasutti (2019) and Taylor et al. (2017) have been removed.